

AN APPLICATION OF THE SPECTRAL KURTOSIS TO MONITOR CONTAINER GANTRY CRANES' MACHINERY

Juan José González de la Rosa, J. M. Sierra, A. Illana, J. A. Carmona, L. M. Calvente
University of Cádiz, Electronics Area, Research Group PAIDI-TIC-168, EPSA
Av. Ramón Puyol S/N, E-11202, Algeciras, Cádiz, Spain

Antonio Moreno Muñoz
University of Córdoba, Electronics Area, Research Group PAIDI-TIC-168
Campus Rabanales, A. Einstein C-2. E-14071, Córdoba, Spain

Keywords: Fault detection, Gantry crane, Higher-Order Statistics, Spectral kurtosis, Transient detection, Vibration monitoring.

Abstract: The Spectral Kurtosis (SK) enhances non-Gaussian behavior associated to deviations from the nominal operation of the cranes machinery. This fact eases fault detection, with the subsequent prevention of dramatic malfunction. In this paper the rotor of a container gantry crane is monitored to get the kurtosis of its normal operation. Then, two types of rolling bearings faults are modeled, according to the design of the rotors crane. These signals are added to the real normal operation recordings, and processed under an estimator of the SK. The experience allows the conformation of a higher-order statistical fault-pattern data base, without the need of stopping huge machinery, and with the subsequent saving, settling the basis of an automatic surveillance system.

1 INTRODUCTION

The study of the vibrations in a gantry crane used in a containers' terminal is an issue related to the security of the crane operators and to the durability of the design. Vibrations take place mostly in the operator's cabin and in the machinery hall; see the photo in Fig. 1 to get a first approximation of the machinery under test.

Numerous achievements have been made in the field of the control for overhead crane systems, which have proven to be an improvement in the position accuracy, safety and stabilization control. To cite: (Ju et al., 2006; Hua and Shine, 2007; Lee et al., 2007). Furthermore, in the work (De la Rosa et al., 2007,), the cabin system has been modeled with *Simulink* and the vibration modes have been separated using the independent component analysis, settling the basis of signal analysis in containers' cranes systems.

In the field of fault diagnosis, numerous improvements have been made, cataloguing faults within big machinery. The vast majority of the advances are based in the traditional power spectral analysis, which



Figure 1: Container Gantry Cranes at Algeciras harbor.

is very sensible to noise and does not offer a complete statistical characterization; in this sense, it is very well known the potential usability of Higher-Order Statistics (HOS) (De la Rosa and Muñoz, 2008,). Among them, it is worthy remarkable the improvement described in (Antoni, 2006) and (Antoni, 2007),

where the Spectral Kurtosis (SK) is applied to vibratory surveillance and diagnostics of rotating machines; faults are modeled herein and characterized using fourth-order statistics.

In this paper, the application of HOS consists of characterizing the normal operation of a crane's rotor. Then, based in this nominal kurtosis, we add two types of modeled faults to the normal operating recordings. These faults are associated to different catalogued defects in the rolling bearings (outer and inner race defects), in order to obtain their characterization based in the SK. The rotor is located in the machine hall of a container crane; so the described fourth-order analysis of the pseudo-synthetic signals, enables characterization without stopping the crane. Faults are modeled according to the dimensions of the rolling bearings.

An intermediate result proves the increment of the non-Gaussian feature of the faults. From the global calculation (numerical) of the kurtosis, we prove that the nominal operation is slightly non-Gaussian, and the kurtosis' increment is associated to faulty bearings. The main results will be concluded looking at the frequency patterns of the faults recordings, and they show the inter-frequency distance associated to both fault types.

The paper is structured as follows. In Section 2 we make a brief summary on the definition of kurtosis; we use an unbiased estimator of the SK, successfully used in (De la Rosa and Muñoz, 2008,), where a higher measurement bandwidth was used. Fault modeling is described in Section 3. Results are presented in Section 4. Finally, conclusions are drawn in Section 5.

2 KURTOSIS AND SPECTRAL KURTOSIS

In statistics, kurtosis is a measure of the "peakedness" of the probability distribution of a random variable X . Higher kurtosis means more of the variance is due to infrequent extreme deviations, as opposed to frequent modestly-sized deviations.

Kurtosis is more commonly defined as the fourth central cumulant divided by the square of the variance of the probability distribution, which is the so-called excess kurtosis, according to Eq. (1):

$$\gamma_2 = \frac{\kappa_4}{\kappa_2^2} = \frac{\mu_4}{\sigma^4} - 3, \quad (1)$$

where $\mu_4 = \kappa_4 + 3\kappa_2^2$ is the 4th-order central moment; and κ_4 is the 4th-order central cumulant, i.d. the ideal value of $Cum_{4,x}(0, 0, 0)$. This definition of

the 4th-order cumulant for zero time-lags comes from a combinational relationship among the cumulants of stochastic signals and their moments, and is given by the *Leonov-Shiryayev* formula. A complete description for these statistics can be found to cite in (Nikias and Mendel, 1993; Mendel, 1991).

The "minus 3" at the end of this formula is a correction to make the kurtosis of the normal distribution equal to zero. Excess kurtosis can range from -2 to $+\infty$.

A high kurtosis distribution has a sharper "peak" and fatter "tails", while a low kurtosis distribution has a more rounded peak with wider "shoulders". Distributions with zero kurtosis are called mesokurtic (e.g. the normal distribution). A distribution with positive kurtosis is called leptokurtic. A leptokurtic distribution has a more acute "peak" around the mean and "fat tails" (e.g. the *Laplace* distribution). A distribution with negative kurtosis is called platykurtic, which has a smaller "peak" around the mean and "thin tails" (e.g. the continuous or discrete uniform distributions, and the raised cosine distribution; the most platykurtic distribution of all is the *Bernoulli* distribution).

In Measurement Science, the sample kurtosis is calculated over a sample-register (an N -point data record), and noted by:

$$g_2 = \frac{m_4}{s^4} - 3 = \frac{m_4}{m_2^2} - 3 = \frac{\frac{1}{N} \sum_{i=1}^N (x_i - \bar{x})^4}{\left[\frac{1}{N^2} \sum_{i=1}^N (x_i - \bar{x})^2 \right]^2} - 3, \quad (2)$$

where m_4 is the fourth sample moment about the mean, m_2 is the second sample moment about the mean (that is, the sample variance), and \bar{x} is the sample mean. The sample kurtosis defined in Eq. (2) is a biased estimator of the population kurtosis, if we consider a sub-set of samples from the population (the observed data).

In the frequency domain, the ideal SK is a representation of the kurtosis of each frequency component of a process (or data from a measurement instrument x_i) (De la Rosa and Muñoz, 2008; Vrabie et al., 2003,). For estimation issues we will consider M realizations of the process; each realization containing N points; i.d. we consider M measurement sweeps, each sweep with N points. The time spacing between points is the sampling period, T_s , of the data acquisition unit.

A biased estimator for the spectral kurtosis and for a number M of N -point realizations at the frequency index m , is given by Eq. (3):

$$\hat{G}_{2,X}^{N,M}(m) = \frac{M}{M-1} \left[\frac{(M+1) \sum_{i=1}^M |X_N^i(m)|^4}{\left(\sum_{i=1}^M |X_N^i(m)|^2 \right)^2} - 2 \right]. \quad (3)$$

This estimator is the one we have implemented in the program code in order to perform the data computation and it was also used successfully in (De la Rosa and Muñoz, 2008,). The estimator converges in probability to the quantity being estimated (the true value, γ_2) when the number of realizations M and the sample size N tend to $+\infty$. So we say that the estimator is asymptotically *consistent* with respect to M and N .

To show the ideal performance of the estimator, which has been described in these lines, and also described in (De la Rosa and Muñoz, 2008,), we show an example based in synthetics. A mix of six different signals have been designed. Each mixture is the sum of a constant-amplitude sine of 2 kHz, a constant-amplitude sine at 9 kHz, a Gaussian-distributed-amplitude sine at 5 kHz, a Gaussian-distributed-amplitude sine at 18 kHz, a Gaussian white noise, and a colored Gaussian noise between 12 and 13 kHz. Each mixture (realization or sample register) contains 1324 points.

Negative kurtosis ("-1") is expected for constant-amplitude processes, positive kurtosis (not bounded peaks) should be associated to random-amplitudes and zero kurtosis will characterize both Gaussian-noise processes. This is proved in Fig. 2, which shows a good performance because enough registers have been averaged ($M=500$).

The SK is supposed to behave similarly with syn-

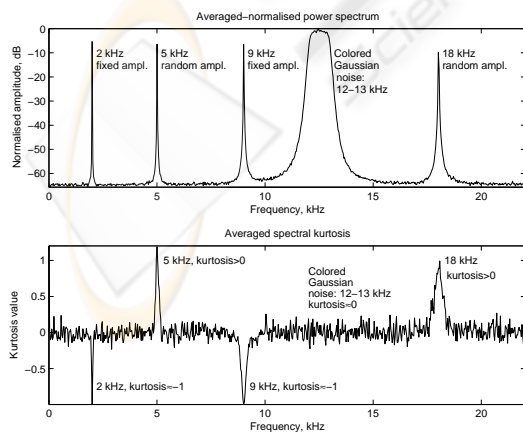


Figure 2: Performance over a set of synthetics, for $M=500$ realizations.

thetics associated to bearing fault modeling. As we find constant amplitude impulses (associated to faults), an infinite succession of "-1" should appear in the SK. This is also taken to measure inter-frequency distances.

3 FAULT MODELING

Bearing components normally fail in the following order: race defects (the most common), ball or roller defects and cage defects (unless the bearing was defective when installed). Inner race defects and failures occur at much lower amplitudes than outer race defects.

BSF (Ball Spin Frequency) is usually generated when a ball or roller is defective. When multiple balls are defective, multiples of BSF appear, i.e., if BSF is at 800 RPM and four balls have defects, you should also see a peak at 3200 RPM or $4 \times$ BSF. In all cases, a surface defect on an inner race, an outer race or on a roller (ball) generates shocks at the bearing characteristic frequencies.

In a frequency spectrum, defects correspond to pulse trains of frequencies extending from the 0-1000 Hz range in the domain of vibratory-acoustics. Such families of peaks merge with the peaks due to other causes. A real specialist must then deal with the bearing analysis to sort out other causes present in the frequency spectrum. In the vibration frequency range (typically 10-1000 Hz), the patterns of frequency spectra may indeed be complex, due to problems of rotor dynamics; pumps ventilators (blade passing frequencies, vanes, etc). This noise (usually Gaussian) can be rejected using HOS.

In the present work, we have modeled the outer race and the inner race faults, which are the most usual. Both faults are modeled with the same impulses' amplitudes. The following modeled magnitudes are exposed according to the jargon's nomenclature. The rotation speed (RPM/60), $f = 1$ Hz; BPFI (Bearing Inner Race Frequency) = 13 Hz; BPFO (Bearing Outer Race Frequency) = 7 Hz; BSF (Ball Spin Frequency) $\cong 1.15$ Hz; FTF (Fundamental Train Frequency) $\cong 0.35$ Hz.

The above magnitudes have been calculated considering the dimensions of the rolling bearing: contact angle (α) = zero; B_d (ball or roller diameter) = 65 mm; P_d (pitch diameter) = 215 mm; N_b (number of balls, or rollers) = 20. The following expressions expanded in Eq. (4), allow calculation for the present situation:

$$\begin{aligned}
 BPFO &= f \times \frac{N_b}{2} \times \left[1 - \frac{Bd}{Pd} \times \cos(\alpha) \right] \\
 BPFI &= f \times \frac{N_b}{2} \times \left[1 + \frac{Bd}{Pd} \times \cos(\alpha) \right] \\
 BSF &= (f/2) \times \frac{Pd}{Bd} \times \left[1 - \frac{Bd}{Pd} \times \cos^2(\alpha) \right] \\
 FTF &= (f/2) \times \frac{Pd}{Bd} \times \left[1 - \frac{Bd}{Pd} \times \cos(\alpha) \right]
 \end{aligned} \quad (4)$$

According to Eq. (4), outer and inner faults have been modeled with the form of impulse trains whose pulse repetition rate obeys the calculation performed in Eq (4). Two sample registers are depicted in Fig. 3.

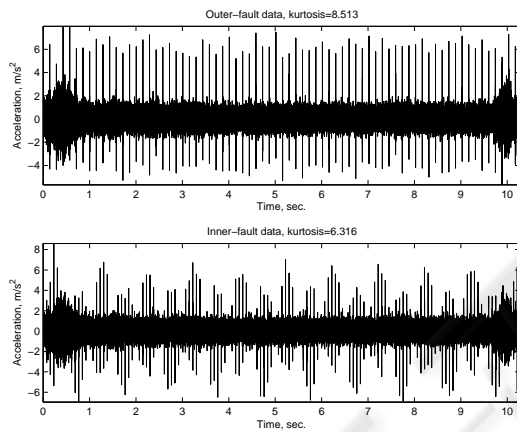


Figure 3: Two data registers which model both types of faults in the rotor's rolling bearings. Impulse repetition: BPFI (Bearing Inner Race Frequency) = 13 Hz; BPFO (Bearing Outer Race Frequency) = 7 Hz.

It is also seen in Fig. 3, the background raw data, which corresponds to normal operation. A *SNR* of 6 dB has been fixed (variance of the normal vibration, 4; variance of the pulse trains 8). According to this model, results for the SK analysis are presented hereinafter.

4 EXPERIMENTS AND RESULTS

We show the experimental location of the sensors in Fig. 4. Three sensors are primarily connected to the rotor carcass, aiming to confirm the similarity of the three signals, in order to reduce the three to one measurement point. The rotor's structure under test is located inside the machine room of the crane (see Fig. 1).

Industrial accelerometers (model KD42V) have been used with a sensitivity of 100 mV/g, which is the usual standard in noise and vibration control Engineering. The sensors' usable bandwidth is of 100 kHz. Despite the fact that low-frequency vibrations are involved, the sampling frequency was set to 10 kHz in order to capture high resolution recordings, aiming to buried them with modeled impulses' trains.

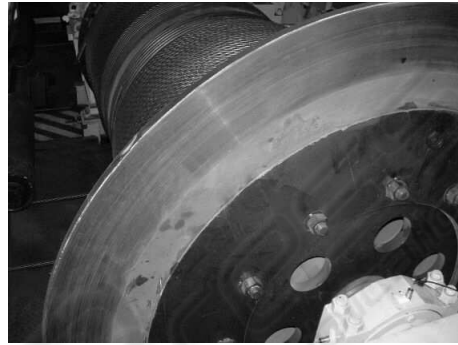


Figure 4: A photograph of the rotor and the location of the sensors.

The kurtosis as a global indicator, considered as the average of the kurtosis computed for each individual frequency component, is not a valid tool to extract features. This is due to the fact that no discrimination is made neither among the frequency bands nor the frequency pattern, from the global point of view.

In order to get a reliable characterization, each register (10 kHz sampled) contains numerous data (102,714; about 10 sec. sampling). In normal operation, the mean value of the excess kurtosis is 1.343, which is somewhat over the Gaussian limit (kurtosis = 0). For the outer fault case, the median of the kurtosis is 8.513. The inner fault is characterized by an average kurtosis of 6.316. This by the way is an indication of the type of fault. But the global indication is very susceptible to errors associated to transients, or other non-Gaussian noise, and does not provide information relative to the frequency bands.

So, the key of the SK detection strategy used in this work, lies in the potential enhancement of the non-Gaussian behavior of the vibrations. If this happens, i.e. if an increase of the non-Gaussian activity (increase in the kurtosis, peakedness of the probability distribution) is observed-measured in the SK graph, there may be deviation from normal functioning.

Fig. 5 shows the frequency analysis associated to one recording, which models an inner race defect in the rotor bearing. At a first glance, it is difficult to reach a frequency pattern, but a closer examination reveals the constant inter-frequency distance which

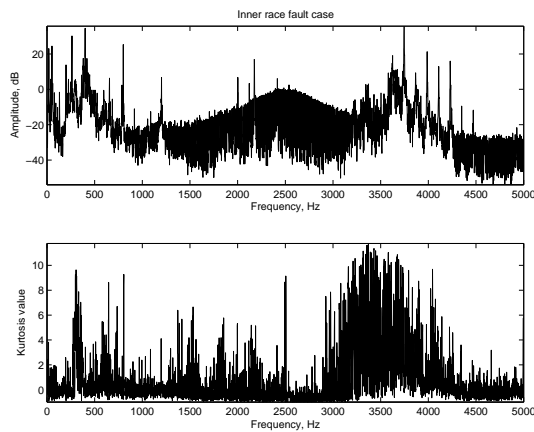


Figure 5: High resolution frequency analysis of an inner race fault.

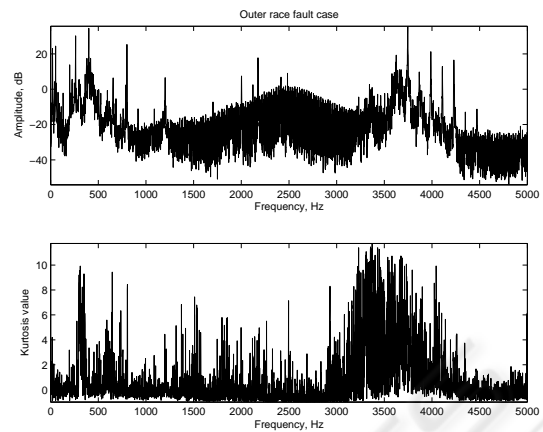


Figure 7: High resolution frequency analysis of a fault in the outer race.

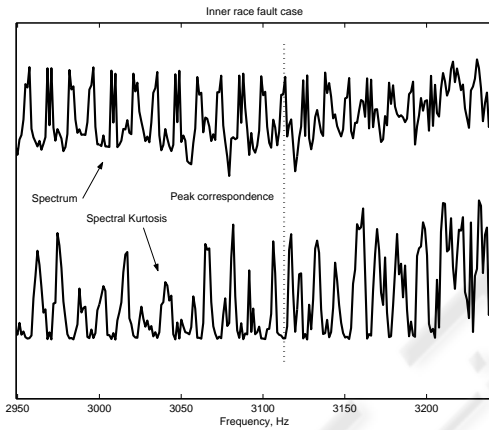


Figure 6: High resolution frequency analysis of an inner race fault. A zoom of Fig. 5. Graphs have been shifted for convenience. Inter-frequency = 13 Hz.

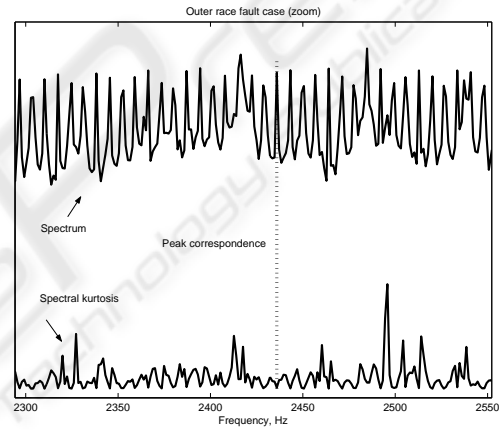


Figure 8: High resolution frequency analysis of an outer race fault. A zoom of Fig. 7. Graphs have been shifted to improve visualization. Inter-frequency = 7 Hz.

characterizes this type of fault.

Fig. 7 presents the spectral analysis of an outer race fault, which is very similar to the inner fault case, depicted in Fig. 6.

On the basis of the second and fourth-order spectra, we conclude the possibilities of the SK to distinguish between two common faults in rotor bearings.

5 CONCLUSIONS AND ACCOMPLISHMENTS

Results show the potential use of the SK to target faults in mechanical systems. Concretely, the estimator of the SK is able to discriminate between two different faults, commonly encountered in rolling bearings, and targeted here via the inter-frequency dis-

tance.

The improved performance of the SK over the global excess kurtosis resides in the possibility of analyzing separated frequency bands, or inter-frequency distances, which are more indicative features of faults than a mere numeric statistical calculation. The kurtosis as a global indicator is considered only a prior indication of the fault.

The interest of the experiment resides in the possibility of incorporate this signal processing algorithm to the engine of an expert system in order to monitor on-site performance of machinery, and get a predictive surveillance. This would be done without stopping production of such big machinery.

REFERENCES

- Antoni, J. (2006). The spectral kurtosis: application to the vibratory surveillance and diagnostics of rotating machines. *Mechanical Systems and Signal Processing* (Ed. Elsevier), 20(2):308–331.
- Antoni, J. (2007). Cyclic spectral analysis in practice. *Mechanical Systems and Signal Processing* (Ed. Elsevier), 21(2):597–630.
- Hua, Y. J. and Shine, Y. K. (2007). Adaptive coupling control for overhead crane systems. *Mechatronics*, (-):in Press.
- Ju, F., Choo, Y., , and Cui, F. (2006). Dynamic response of tower crane induced by the pendulum motion of the payload. *International Journal of Solids and Structures*, (43):376–389.
- Lee, D.-H., Cao, Z., and Meng, Q. (2007). Scheduling of two-transtainer systems for loading outbound containers in port container terminals with simulated annealing algorithm. *Int. J. Production Economics*, (-):in Press.
- Mendel, J. M. (1991). Tutorial on higher-order statistics (spectra) in signal processing and system theory: Theoretical results and some applications. *Proceedings of the IEEE*, 79(3):278–305.
- Nikias, C. L. and Mendel, J. M. (1993). Signal processing with higher-order spectra. *IEEE Signal Processing Magazine*, pages 10–37.
- De la Rosa, J. J. G. and Muñoz, A. M. (2008). Higher-order cumulants and spectral kurtosis for early detection of subterranean termites. *Mechanical Systems and Signal Processing* (Ed. Elsevier), 22(Issue 1):279–294. Available online 1 September 2007.
- De la Rosa, J. J. G., Puntonet, C. G., Moreno, A., Illana, A., and Carmona, J. A. (2007). An application of ICA to BSS in a container gantry crane cabin's model. *Lecture Notes in Computer Science (LNCS)*, 4666:714–721. 7th International Conference on Independent Component Analysis and Signal Separation (ICA 2007) London, UK, September 9-12, 2007, Proceedings.
- Vrabie, V., Granjon, P., and Serviere, C. (2003). Spectral kurtosis: from definition to application. In IEEE, editor, *IEEE-EURASIP International Workshop on Non-linear Signal and Image Processing (NSIP'2003)*, volume 1, pages 1–5.